

# Iron-Catalyzed Cross-Electrophile Coupling for the Formation of All-Carbon Quaternary Centers

Andria L. Pace, Felix Xu, Wei Liu, Marissa N. Lavagnino, and David W. C. MacMillan\*

Cite This: <https://doi.org/10.1021/jacs.4c14942>

Read Online

ACCESS |



Metrics &amp; More



Article Recommendations



Supporting Information

**ABSTRACT:** Quaternary carbon centers are desirable targets for drug discovery and complex molecule synthesis, yet the synthesis of these motifs within traditional cross-coupling paradigms remains a significant challenge due to competing  $\beta$ -hydride elimination pathways. In contrast, the bimolecular homolytic substitution ( $S_H2$ ) mechanism offers a unique and attractive alternative pathway. Metal porphyrin complexes have emerged as privileged catalysts owing to their ability to selectively form primary metal–alkyl complexes, thereby eliminating the challenges associated with tertiary alkyl complexation with a metal center. Herein, we report an iron-catalyzed cross-electrophile coupling of tertiary bromides and primary alkyl electrophiles for the formation of all-carbon quaternary centers through a biomimetic  $S_H2$  mechanism.

Quaternary carbon centers are ubiquitous in natural products,<sup>1</sup> pharmaceuticals,<sup>2</sup> and bioactive molecules,<sup>3</sup> yet the construction of these motifs remains a significant challenge.<sup>4</sup> Quaternary centers are not readily forged through traditional cross-coupling platforms that employ reductive elimination mechanisms because of competing  $\beta$ -hydride elimination resulting from interaction of the tertiary coupling partner with the metal center for 4d and 5d transition metals.<sup>5</sup> Recent work from our laboratory has led to the development of a suite of metal complexes capable of “sorting” alkyl components in solution as a means to overcome the problem of  $\beta$ -hydride elimination.<sup>6</sup> Under this paradigm, termed “radical sorting,”<sup>7</sup> primary and tertiary radicals are formed in solution, and the metal catalyst selectively binds the primary radical in preference to the tertiary radical due to the enhanced M–C bond strength of the resultant primary alkyl–metal complex.<sup>8</sup> This complex is poised to undergo bimolecular homolytic substitution ( $S_H2$ ) to forge the C–C bond. Our laboratory and others<sup>9</sup> have found this  $S_H2$  bond-forming mechanism to be a useful strategy for the incorporation of C( $sp^3$ )-rich functionality.<sup>10</sup>

Under this paradigm, orthogonal activation of different functional groups is employed to achieve redox-neutral cross-coupling. Therefore, this “radical sorting” approach is highly effective in redox cycles wherein two radicals are formed in solution via photocatalyst-mediated activation and then sorted by a metal catalyst;<sup>11</sup> however, we envisioned extending this concept to a single functional group cross-coupling (Figure 1A). We reasoned that this objective might be achieved via the direct nucleophilic substitution of a primary electrophile by the metal catalyst, thereby circumventing the need to generate a primary radical intermediate (Figure 1B). This is in contrast to radical capture mechanisms for the formation of metal–alkyl complexes, which have been explored within the metal-laphotoredox regime.<sup>12</sup> Such a nucleophilic activation mechanism would expand the scope of primary electrophiles to encompass substrates susceptible to  $S_N2$ -type mechanisms,

such as mesylate (OMs) and tosylate (OTs) electrophiles (Figure 1C).<sup>13</sup> Although this type of reactivity has been shown with cobalt-based catalytic systems,<sup>14</sup> iron has been comparably underexplored beyond seminal studies carried out in the 1980s by Savéant and co-workers,<sup>15</sup> which elegantly demonstrated the feasibility of iron-mediated  $S_N2$  reactions of primary bromides with an electrochemically generated reduced-state iron(I) complex.<sup>16</sup> Application of iron-mediated  $S_N2$  reactivity toward catalytic cross-coupling remains underdeveloped. We envisioned combining this  $S_N2$ -type activation mechanism with subsequent  $S_H2$  bond formation to develop a new approach to accessing quaternary-coupled products (Figure 1D).

An advantage of the  $S_H2$  mechanism is the fact that bond formation is often agnostic to the identity of the starting material. Execution of the proposed cross-coupling platform could potentially enable the construction of all-carbon quaternary centers from a variety of precursors, thereby vastly expanding the accessible chemical space. Specifically, we envisioned merging  $S_N2$  substrate activation with  $S_H2$  bond formation in a cross-electrophile coupling to form new quaternary centers.<sup>17</sup> Cross-electrophile coupling reactions have been extensively explored and found to be generally mild and modular in nature.<sup>18</sup> Therefore, we envisioned cross-electrophile coupling to be ideally suited to our goal of orthogonal functional group activation. As outlined in Table 1, the proposed mechanism would proceed as follows: visible light excitation of the Ir photocatalyst (**1**) generates a long-lived triplet excited state ( $\tau = 1.1 \mu s$ ).<sup>19</sup> Single-electron

Received: October 24, 2024

Revised: November 14, 2024

Accepted: November 15, 2024

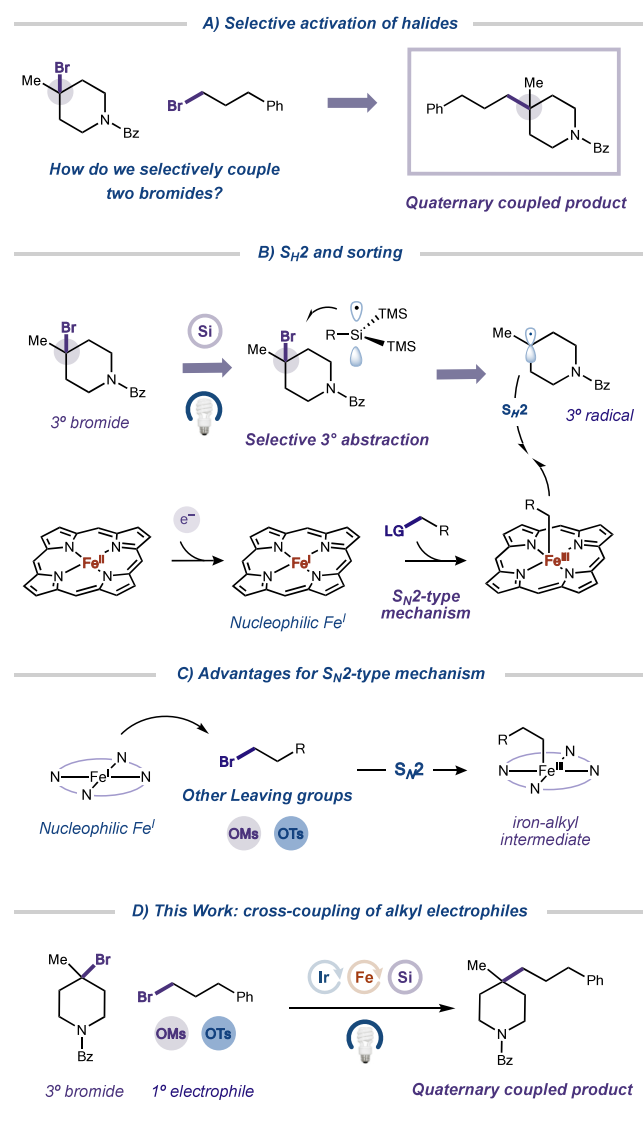
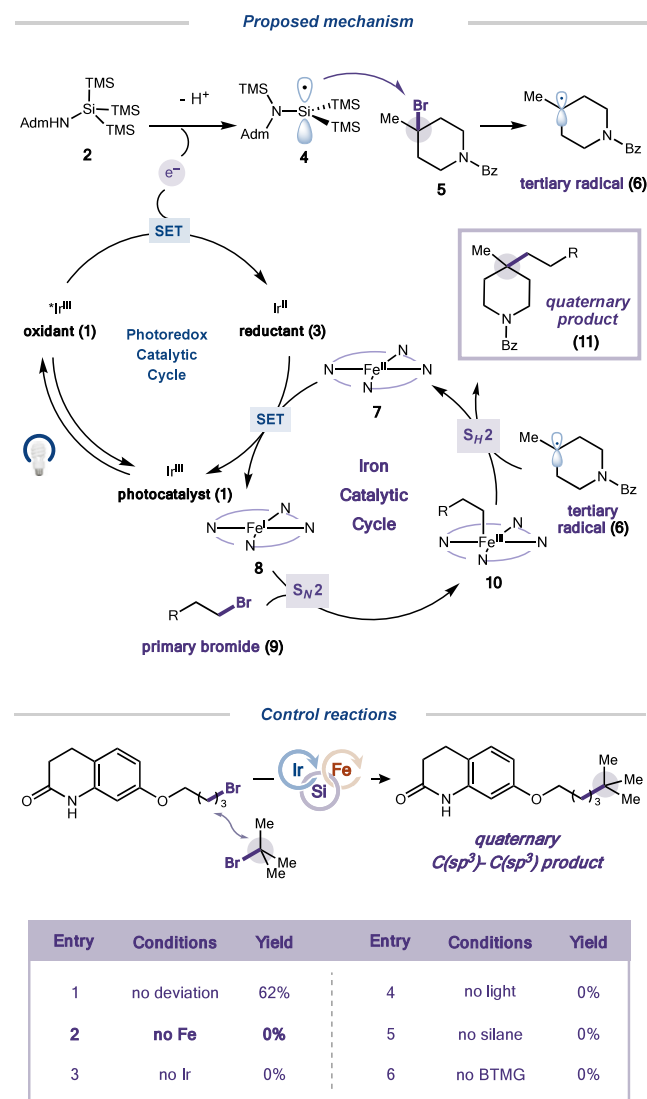


**Figure 1.** Selective activation of alkyl halides toward cross-coupling via bimolecular homolytic substitution ( $S_H2$ ).

oxidation of the adamantyl aminosilane reagent (**2**) by the excited-state photocatalyst affords the reduced Ir(II) complex (**3**).<sup>20</sup> Subsequent aza-Brook rearrangement of the aminosilane reagent affords the silyl radical intermediate (**4**) poised to undergo halogen atom transfer (XAT) with the tertiary bromide substrate (**5**) to afford the corresponding tertiary radical intermediate (**6**).<sup>21</sup> The reduced-state Ir(II) complex (**3**) then performs a single-electron reduction of the Fe(II)-(OEP) (OEP, octaethylporphyrinato) catalyst (**7**) [ $E^\circ[Fe(II)/Fe(I)] = -1.23$  V vs SCE in DMF]<sup>16</sup> to afford the highly nucleophilic Fe(I)(OEP) species (**8**) and regenerate the Ir(III) photocatalyst (**1**). The Fe(I)(OEP) is proposed to undergo an  $S_N2$ -type reaction with the primary alkyl coupling partner (**9**) to afford the key Fe(III)-alkyl intermediate (**10**),<sup>16,22</sup> which can undergo  $S_H2$  bond formation to deliver the cross-coupled product (**11**) and regenerate the Fe(II)(OEP) catalyst (Table 1).

We were pleased to find that the proposed reactivity could be achieved using primary and tertiary alkyl bromide coupling partners (Table 1, entry 1). Control reactions indicated that all components are necessary to achieve reactivity (entries 2–6).

**Table 1. Mechanism and Control Reactions<sup>a</sup>**

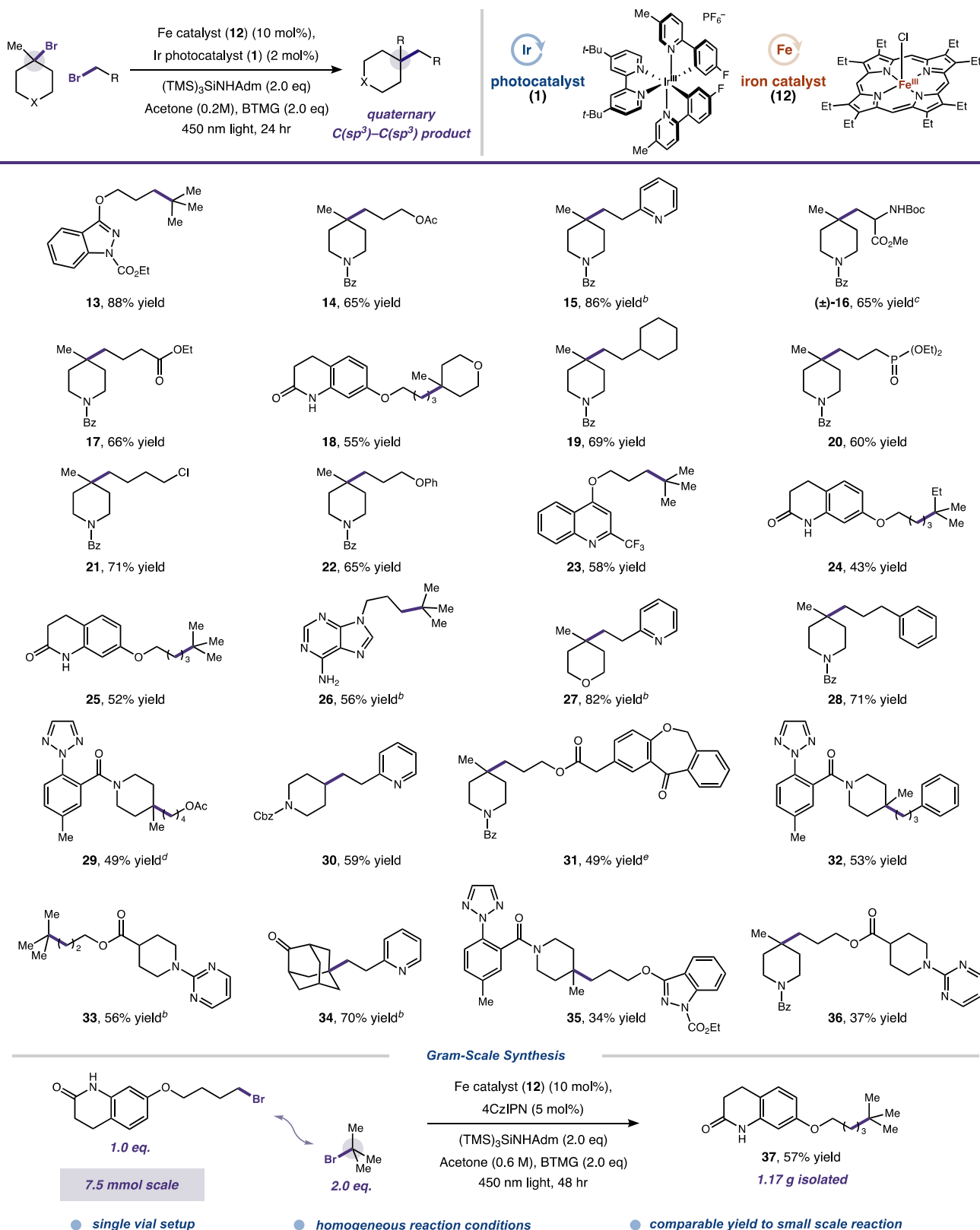


<sup>a</sup>Control reactions performed with primary bromide (0.05 mmol, 1.0 equiv), tertiary bromide (2.0 equiv), adamantyl aminosilane (**2**) (2.0 equiv), BTMG (2.0 equiv), Fe(OEP)Cl (**12**) (10 mol %), Ir Photocatalyst (**1**) (2 mol %), and acetone (0.2 M) (Entry 1) with deviations as noted (Entries 2–6). Yields determined by UHPLC analysis with methyl benzoate as an internal standard. OEP = octaethylporphyrin. See Supporting Information for experimental details.

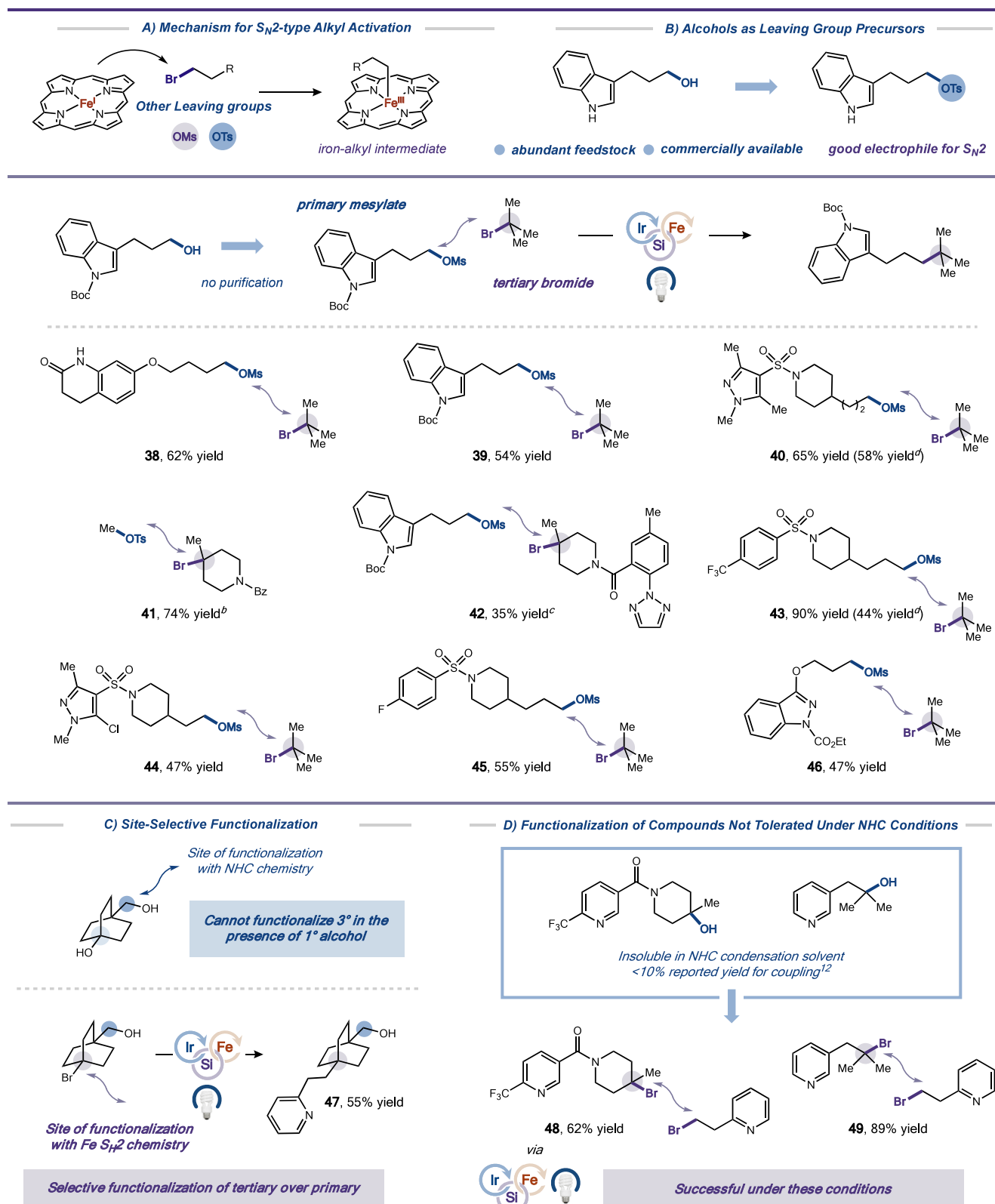
Notably, no product is formed in the absence of an iron catalyst (entry 2). In  $S_H2$  systems that generate two radical species, small amounts of background product are formed in the no-metal control reactions due to statistical radical–radical coupling, yet none is observed in this system.<sup>7,8,12</sup>

With optimized conditions established (Table 1, entry 1), we evaluated the scope of the transformation (Table 2). Primary bromides containing indazole (**13**, 88% yield), acetate (**14**, 65% yield), pyridine (**15**, 86% yield), and protected amino acid (**16**, 65% yield) functionality were well-tolerated.

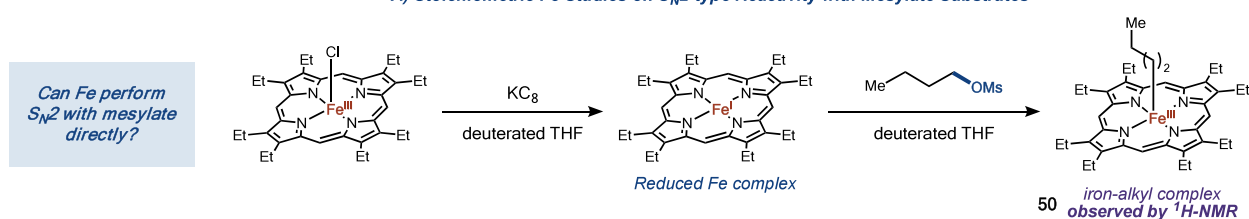
Furthermore, bifunctional electrophilic linkers (**17**, 66% yield and **21**, 71% yield) were effective, demonstrating selectivity for halide alkylation. Coupling with a variety of heterocycles (**18–23**, 55–69% yield) proceeded in good to

Table 2. Scope of Bromide–Bromide Cross-Electrophile Coupling<sup>a</sup>

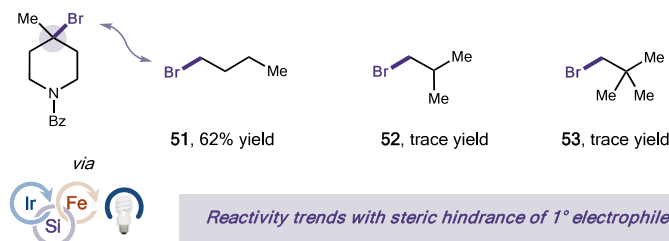
<sup>a</sup>Reactions were performed on a 0.50 mmol scale with primary bromide (0.50 mmol), tertiary bromide (2.0 equiv), adamantyl aminosilane (2.0 equiv), 2-*tert*-butyl-1,1,3,3-tetramethylguanidine (BTMG) (2.0 equiv), Fe(OEP)Cl (2) (10 mol %), Ir photocatalyst (1) (2 mol %), and acetone (0.2 M). The reactions were irradiated with blue LEDs for 24 h at 100% light intensity. <sup>b</sup>BTMG (4.0 equiv). <sup>c</sup>Reaction was performed on a 0.1 mmol scale. <sup>d</sup>Reaction time was 48 h. <sup>e</sup>Light intensity was 25%.

Table 3. Scope of Alcohol–Bromide Cross-Electrophile Coupling<sup>a</sup>

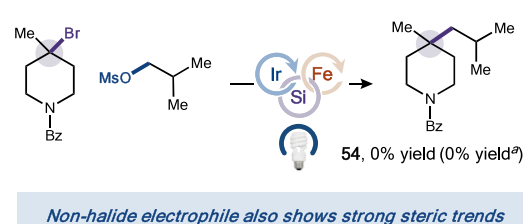
<sup>a</sup>Reactions were performed on a 0.50 mmol scale with primary mesylate/tosylate (0.50 mmol), tertiary bromide (2.0 equiv), adamantyl aminosilane (2.0 equiv), BTMG (2.0 equiv), Fe(OEP)Cl (10 mol %), tetrabutylammonium bromide (TBAB, 1.0 equiv), Ir photocatalyst (**1**) (2 mol %), and acetone (0.2 M). The reactions were irradiated with 450 nm LEDs for 24 h at 25–100% light intensity. <sup>b</sup>Tertiary bromide (0.50 mmol), primary mesylate/tosylate (2.0 equiv), no TBAB additive. <sup>c</sup>Tertiary bromide (0.50 mmol), primary mesylate/tosylate (2.0 equiv), TBAB (2.0 equiv). <sup>d</sup>Yield of the reaction without TBAB additive.

A) Stoichiometric Fe Studies on  $S_N2$ -type Reactivity with Mesylate Substrates

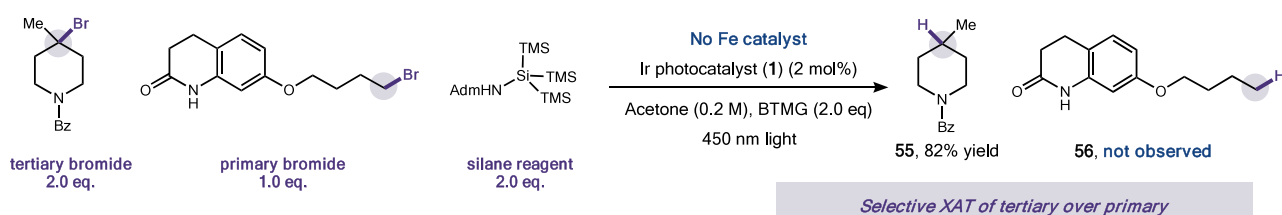
## B) Steric Series Bromides



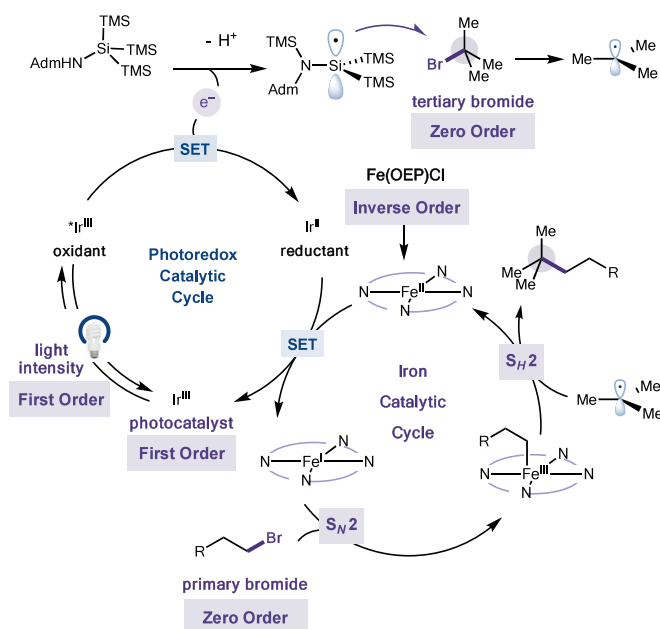
## C) Steric Series Mesylate



## D) Silane Competition Experiment



## E) VTNA Analysis



## F) PhotoNMR Experiment

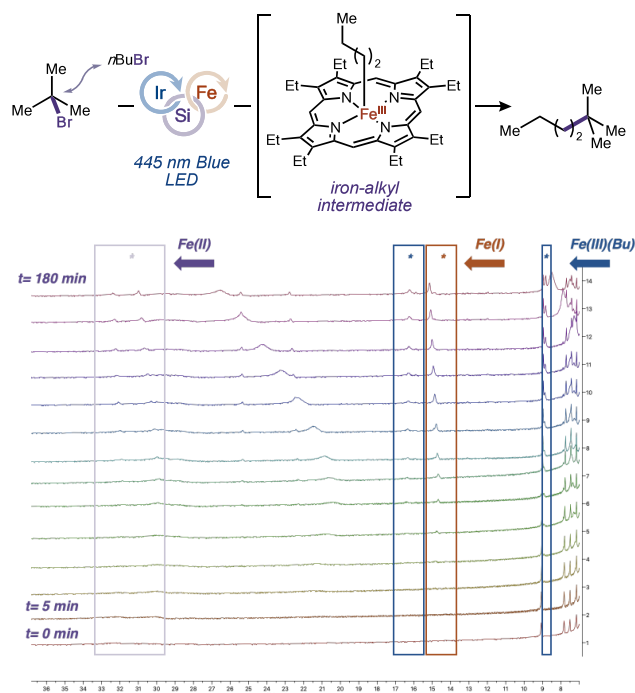


Figure 2. Mechanistic analysis and stoichiometric studies. <sup>a</sup>Performed with TBAB additive.

excellent yield. The quinolone fragment from the pharmaceutical aripiprazole was alkylated in good yield (24, 43% yield and 25, 52% yield), illustrating the power of this method to rapidly install *tert*-butyl groups onto medically relevant molecules, a modification that can modulate compound solubility and other

pharmacokinetic properties.<sup>23</sup> Notably, the nucleobase adenine underwent alkylation (26, 56% yield), thereby demonstrating compatibility with unprotected N–H bonds. Additionally, the reaction tolerates a range of tertiary bromides containing pharmaceutically relevant heterocycles (27–36, 49–82%



yield). Secondary bromides also afford products in good yield (**30**, 59% yield; see the [Supporting Information](#) for additional examples). We observed efficient coupling of the aryl triazole fragment of orexin receptor antagonist, suvorexant (**35**, 34% yield), and the core of the anti-inflammatory agent, isoxepac (**31**, 49% yield). The latter example demonstrates the tolerance of benzophenone functionality in this photoredox regimen. Finally, we envisioned that this method could be particularly amenable to gram-scale synthesis. Previously reported  $S_H2$  reactions utilize heterogeneous bases, which can be problematic for photocatalytic reactions at scale. Additionally, dilute conditions necessitate specialty setups to accommodate scale-up. Our cross-electrophile reaction, in contrast, utilizes a homogeneous base and concentrated conditions, which makes it especially amenable to scale-up (**37**, 57% yield, 1.17 g isolated).

As a feature of our design, we anticipated that primary alkyl substrates bearing a variety of electrophilic leaving groups might be leveraged in the cross-coupling because of the  $S_N2$ -type nature of iron-alkyl formation. In particular, alcohols—a structurally diverse class of abundant feedstocks with wide commercial availability—could serve as attractive cross-coupling precursors.<sup>11,12,24</sup> To this end, we investigated alkyl sulfonates generated from alcohols in one step without purification as primary coupling partners ([Table 3](#)). A variety of primary mesylates containing heterocyclic fragments (**38–40**, 54–65% yield) efficiently furnished quaternary products under this protocol. Methylation was achieved in excellent yield using commercially available methyl tosylate (**41**, 74% yield), and additional heterocyclic fragments were coupled in synthetically useful yield (**42–46**, 35–90% yield). Notably, heteroaryl halides are tolerated (**44**, 47% yield), which demonstrates the selectivity of XAT reagents for tertiary alkyl halides over aryl halides.<sup>25</sup> Furthermore, the reaction proceeded in good to moderate yield in the absence of bromide additive (**40**, 58% yield and **43**, 44% yield; see the [Supporting Information](#) for discussion of the bromide effect). Overall, the  $S_N2$  reactivity demonstrated herein underscores both the mechanistic novelty and the synthetic utility of this reaction, enabling facile cross-coupling to form quaternary carbon centers from alcohol precursors.

We next explored previously unattainable applications of  $S_H2$  technology. Our group has introduced deoxygenative alkylation and arylation procedures that utilize benzoxazolium salts, termed “NHC salts,” to achieve selectivity for primary activation over tertiary activation in diol substrates.<sup>12</sup> We similarly demonstrated selective activation of a bromoalcohol substrate wherein the tertiary bromide was functionalized in the presence of a primary alcohol to deliver the desired product (**47**, 55% yield). Additionally, substrates suffering from poor solubility in the NHC–alcohol condensation procedure,<sup>11,12</sup> when converted to the bromide, afforded product in excellent yield (**48**, 62% yield and **49**, 89% yield).

We next set out to probe the mechanistic aspects of this cross-electrophile coupling, as this catalytic system features key differences from previous  $S_H2$  platforms. The ability to form iron-alkyl complexes through multiple mechanisms has the potential to expand our mechanistic understanding and the synthetic reach of  $S_H2$  reaction development.<sup>26</sup>

Previous reports demonstrated the ability to form primary Fe(OEP)(alkyl) complexes (ex situ using organometallic reagents) and studied their reactivity toward  $S_H2$  bond formation in the presence of tertiary radicals.<sup>6</sup> Building upon

this precedent, we envisioned stoichiometric formation of the Fe-alkyl via the reaction of a preformed Fe(I)(OEP) with a primary mesylate. Observation of the Fe-alkyl complex **50** thus demonstrates the feasibility of Fe(I)  $S_N2$  activation of mesylates en route to Fe-alkyl complexes ([Figure 2A](#)). We also report a strong steric effect on reactivity of primary bromide coupling partners ([Figure 2B](#)), as well as a strong effect for nonhalide electrophiles ([Figure 2C](#)).<sup>27</sup> These results taken together are consistent with an  $S_N2$ -type activation mechanism rather than a primary XAT mechanism.<sup>28</sup>

From the outset, we envisioned that this mechanistic paradigm might allow for the selective and orthogonal activation of two seemingly identical functional groups toward cross-coupling because of the preference of silyl radical XAT for tertiary bromides and the preference of Fe– $S_N2$  for primary electrophiles. For tris(trimethylsilyl)silane, abstraction of a tertiary bromide is on the order of  $1 \times 10^8 \text{ M}^{-1} \text{ s}^{-1}$ , while the rate of XAT for a primary bromide is on the order of  $2 \times 10^7 \text{ M}^{-1} \text{ s}^{-1}$ .<sup>29</sup> Using these values as a benchmark, we set out to investigate the selectivity of XAT under our conditions using an aminosilane reagent. We designed a competition experiment ([Figure 2D](#)) to mimic our reaction stoichiometries. Iron catalyst is omitted to allow direct observation of the ratio of primary/tertiary XAT. Notably, no primary bromide abstraction is observed, which reveals preferential abstraction of tertiary bromide over primary bromide; the difference in XAT rate is indeed sufficient to achieve selectivity. Furthermore, this result implies that a mechanism involving primary bromide XAT is unlikely under these conditions and stoichiometries, consistent with our mechanistic proposal.

Finally, we undertook kinetic and photonuclear magnetic resonance (PhotoNMR) studies to evaluate the speciation of iron catalyst ([Figure 2E,F](#)). The reaction mixture was irradiated with blue light, while paramagnetic  $^1\text{H}$  NMR spectra were collected. The presence of primary Fe(OEP)Bu complex was confirmed via comparison with literature values.<sup>6</sup> We observed a characteristic peak at 14 ppm in the paramagnetic PhotoNMR spectra corresponding to reports for Fe(I)(OEP) complexes.<sup>30</sup> To corroborate this finding, we independently synthesized the Fe(I)(OEP) complex ([Supporting Information Figure S12](#)) via the reduction of Fe(OEP)Cl precatalyst. Observation of an Fe(I)(OEP) complex in solution, which grows in prior to Fe(III)-alkyl formation, is in accord with our mechanistic proposal of  $S_N2$ -type activation of the primary alkyl coupling partner to form the key Fe(III)-alkyl intermediate.

In summary, we report a cross-electrophile approach to quaternary center formation via a biomimetic  $S_H2$  bond formation mechanism. Furthermore, we disclose evidence in support of an  $S_N2$ -type activation of primary alkyl electrophiles invoking a highly nucleophilic Fe(I) species. Such a mechanism, while known for stoichiometric reactions, has been comparably underutilized within the photocatalytic realm. Given the importance of quaternary carbon centers in bioactive compounds, we anticipate that this reaction will find broad use across the synthetic community.

## ■ ASSOCIATED CONTENT

### Supporting Information

The Supporting Information is available free of charge at <https://pubs.acs.org/doi/10.1021/jacs.4c14942>.

Additional experimental results, mechanistic discussion, characterization data, and NMR spectra (PDF)

## AUTHOR INFORMATION

### Corresponding Author

David W. C. MacMillan — Merck Center for Catalysis at Princeton University, Princeton, New Jersey 08544, United States; [orcid.org/0000-0001-6447-0587](https://orcid.org/0000-0001-6447-0587); Email: [dmacmill@princeton.edu](mailto:dmacmill@princeton.edu)

### Authors

Andria L. Pace — Merck Center for Catalysis at Princeton University, Princeton, New Jersey 08544, United States; [orcid.org/0000-0001-8025-1579](https://orcid.org/0000-0001-8025-1579)

Felix Xu — Merck Center for Catalysis at Princeton University, Princeton, New Jersey 08544, United States

Wei Liu — Merck Center for Catalysis at Princeton University, Princeton, New Jersey 08544, United States

Marissa N. Lavagnino — Merck Center for Catalysis at Princeton University, Princeton, New Jersey 08544, United States; [orcid.org/0000-0001-6851-919X](https://orcid.org/0000-0001-6851-919X)

Complete contact information is available at:  
<https://pubs.acs.org/10.1021/jacs.4c14942>

### Notes

The authors declare the following competing financial interest(s): D.W.C.M. declares a competing financial interest with respect to the integrated photoreactor.

## ACKNOWLEDGMENTS

Research reported in this work was supported by the National Institute of General Medical Sciences of the National Institutes of Health (R35GM134897), the Princeton Catalysis Initiative, and kind gifts from Merck, Pfizer, Janssen, Bristol Myers Squibb, Genentech, and Genmab. A.L.P. thanks Princeton University, E. Taylor, and the Taylor family for an Edward C. Taylor Fellowship and the National Science Foundation for a predoctoral fellowship (Award DGE-2039656). F.X. thanks Princeton University for a Charles A. Leach, II Research Fellowship and the Princeton University Office of Undergraduate Research for a summer research fellowship. The content is solely the responsibility of the authors and does not necessarily represent the official views of NIGMS. The authors thank Kenith Conover for assistance with PhotoNMR experiments, Rebecca Lambert for editorial assistance in the preparation of this manuscript, and Dr. Colin Gould for helpful discussions.

## REFERENCES

- (1) Xin, Z.; Wang, H.; He, H.; Gao, S. Recent Advances in the Total Synthesis of Natural Products Bearing the Contiguous All-Carbon Quaternary Stereocenters. *Tetrahedron Lett.* **2021**, *71*, 153029.
- (2) Talele, T. Opportunities for Tapping into the Three-Dimensional Chemical Space through a Quaternary Carbon. *J. Med. Chem.* **2020**, *63*, 13291–13315.
- (3) Peterson, E.; Overman, L. Contiguous Stereogenic Quaternary Carbons: A Daunting Challenge in Natural Products Synthesis. *Proc. Natl. Acad. Sci. U.S.A.* **2004**, *101*, 11943–11948.
- (4) Quasdorf, K. W.; Overman, L. E. Catalytic Enantioselective Synthesis of Quaternary Carbon Stereocenters. *Nature* **2014**, *516*, 181–191.
- (5) Choi, J.; Fu, G. Transition Metal-Catalyzed Alkyl-Alkyl Bond Formation: Another Dimension in Cross-Coupling Chemistry. *Science* **2017**, *356*, No. eaaf7230.

- (6) Liu, W.; Lavagnino, M. N.; Gould, C. A.; Alcázar, J.; MacMillan, D. W. C. A Biomimetic  $S_H2$  Cross-Coupling Mechanism for Quaternary  $sp^3$ -Carbon Formation. *Science* **2021**, *374*, 1258–1263.
- (7) Tsybal, A. V.; Bizzini, L. D.; MacMillan, D. W. C. Nickel Catalysis via  $S_H2$  Homolytic Substitution: The Double Decarboxylative Cross-Coupling of Aliphatic Acids. *J. Am. Chem. Soc.* **2022**, *144*, 21278–21286.
- (8) Sakai, H. A.; MacMillan, D. W. C. Nontraditional Fragment Coupling of Alcohols and Carboxylic Acids:  $C(sp^3)$ - $C(sp^3)$  Cross-Coupling via Radical Sorting. *J. Am. Chem. Soc.* **2022**, *144*, 6185–6192.
- (9) Gan, X.-c.; Kotesova, S.; Castanedo, A.; Green, S.; Möller, S.; Shen, R. Iron-Catalyzed Hydrobenzylation: Stereoselective Synthesis of (–)-Eugenol. *J. Am. Chem. Soc.* **2023**, *145*, 15714–15720.
- (10) Mao, E.; MacMillan, D. W. C. Late-Stage  $C(sp^3)$ -H Methylation of Drug Molecules. *J. Am. Chem. Soc.* **2023**, *145*, 2787–2793.
- (11) Gould, C.; Pace, A.; MacMillan, D. W. C. Rapid and Modular Access to Quaternary Carbons from Tertiary Alcohols via Bimolecular Homolytic Substitution. *J. Am. Chem. Soc.* **2023**, *145*, 16330–16336.
- (12) Chen, R.; Intermaggio, N.; Xie, J.; Rossi-Ashton, J.; Gould, C.; Martin, R.; Alcázar, J.; MacMillan, D. W. C. Alcohol-Alcohol Cross-Coupling Enabled by  $S_H2$  Radical Sorting. *Science* **2024**, *383*, 1350–1357.
- (13) Hamlin, T. A.; Swart, M.; Bickelhaupt, F. M. Nucleophilic Substitution ( $S_N2$ ): Dependence on Nucleophile, Leaving Group, Central Atom, Substituents, and Solvent. *ChemPhysChem* **2018**, *19*, 1315–1330.
- (14) (a) Komeyama, K.; Michiyuki, T.; Osaka, I. Nickel/Cobalt-Catalyzed  $C(sp^3)$ - $C(sp^3)$  Cross-Coupling of Alkyl Halides with Alkyl Tosylates. *ACS Catal.* **2019**, *9*, 9285–9291. (b) Zhang, Q.; van der Donk, W.; Liu, W. Radical-Mediated Enzymatic Methylation: A Tale of Two SAMs. *Acc. Chem. Res.* **2012**, *45*, 555–564.
- (15) (a) Arasasingham, R.; Balch, A.; Cornman, C.; Latos-Grazynski, L. Dioxygen Insertion into Iron(III)-Carbon Bonds. NMR Studies of the Formation and Reactivity of Alkylperoxo Complexes of Iron(III) Porphyrins. *J. Am. Chem. Soc.* **1989**, *111*, 4357–4363. (b) Lexa, D.; Savéant, J.-M.; Su, K.; Wang, D. Chemical vs. Redox Catalysis of Electrochemical Reactions. Reduction of trans-1,2-Dibromocyclohexane by Electrogenated Aromatic Anion Radicals and Low Oxidation State Metalloporphyrins. *J. Am. Chem. Soc.* **1987**, *109*, 6464–6470. (c) Lexa, D.; Savéant, J.-M.; Wang, D. Electroreductive Alkylation of Iron Porphyrins. Iron(III), Iron(II), and Iron(I) Alkyl Complexes from the Reaction of Doubly Reduced Iron(II) Porphyrins with Alkyl Halides. *Organometallics* **1986**, *5*, 1428–1434.
- (16) Lexa, D.; Mispelter, J.; Savéant, J.-M. Electroreductive Alkylation of Iron in Porphyrin Complexes. Electrochemical and Spectral Characteristics of  $\sigma$ -Alkyliron Porphyrins. *J. Am. Chem. Soc.* **1981**, *103*, 6806–6812.
- (17) (a) Knappe, C. E.; Grupe, S.; Gartner, D.; Corpet, M.; Gosmini, C.; Jacobi von Wangelin, A. Reductive Cross-Coupling Reactions Between Two Electrophiles. *Chem.—Eur. J.* **2014**, *20*, 6828–6842. (b) Weix, D. J. Methods and Mechanisms for Cross-Electrophile Coupling of  $Csp^2$  Halides with Alkyl Electrophiles. *Acc. Chem. Res.* **2015**, *48*, 1767–1775. (c) Smith, R.; Zhang, X.; Rincón, J.; Agejas, J.; Mateos, C.; Barberis, M.; García-Cerrada, S.; de Frutos, O.; MacMillan, D. W. C. Metallaphotoredox-Catalyzed Cross-Electrophile  $Csp^3$ - $Csp^3$  Coupling of Aliphatic Bromides. *J. Am. Chem. Soc.* **2018**, *140*, 17433–17438.
- (18) (a) Xue, W.; Jia, X.; Wang, X.; Tao, X.; Yin, Z.; Gong, H. Nickel-catalyzed formation of quaternary centers using tertiary electrophiles. *Chem. Soc. Rev.* **2021**, *50*, 4162–4184. (b) Li, P.; Zhu, Z.; Guo, C.; Kou, G.; Wang, S.; Xie, P.; Ma, D.; Feng, T.; Wang, Y.; Qiu, Y. Nickel-electrocatalyzed  $C(sp^3)$ - $C(sp^3)$  cross-coupling of unactivated alkyl halides. *Nature Catalysis* **2024**, *7*, 412–421. (c) Ibrahim, M.; Cumming, G.; Gonzalez de Vega, R.; Garcia-Losada, P.; de Frutos, O.; Kappe, C.; Cantillo, D. Electrochemical Nickel-Catalyzed  $C(sp^3)$ - $C(sp^3)$  Cross-Coupling of Alkyl Halides with Alkyl Tosylates. *J. Am. Chem. Soc.* **2023**, *145* (31), 17023–

17028. (d) Hamby, T.; Lalama, M.; Sevov, C. Controlling Ni Redox States by Dynamic Ligand Exchange for Electroreductive  $C(sp^3)$ – $C(sp^2)$  Coupling. *Science* **2022**, 376, 410–416. (e) Everson, D. A.; Weix, D. J. Cross-Electrophile Coupling: Principles of Reactivity and Selectivity. *J. Org. Chem.* **2014**, 79 (11), 4793–4798. (f) Zhang, W.; Lu, L.; Zhang, W.; Wang, Y.; Ware, S.; Mondragon, J.; Rein, J.; Strotman, N.; Lehnher, D.; See, K.; Lin, S. Electrochemically Driven Cross-Electrophile Coupling of Alkyl Halides. *Nature* **2022**, 604, 292–297. (g) Liu, J.; Ye, Y.; Sessler, J.; Gong, H. Cross-Electrophile Couplings of Activated and Sterically Hindered Halides and Alcohol Derivatives. *Acc. Chem. Res.* **2020**, 53, 1833–1845.

(19) Lowry, M.; Goldsmith, J.; Slinker, J.; Rohl, R.; Pascal, R.; Malliaras, G.; Bernhard, S. Single-Layer Electroluminescent Devices and Photoinduced hydrogen Production from an Ionic Iridium(III) Complex. *Chem. Mater.* **2005**, 17, 5712–5719.

(20) Sakai, H.; Liu, W.; Le, C.; MacMillan, D. W. C. Cross-Electrophile Coupling of Unactivated Alkyl Chlorides. *J. Am. Chem. Soc.* **2020**, 142, 11691–11697.

(21) Zhang, P.; Le, C.; MacMillan, D. W. C. Silyl Radical Activation of Alkyl Halides in Metallaphotoredox Catalysis: A Unique Pathway for Cross-Electrophile Coupling. *J. Am. Chem. Soc.* **2016**, 138, 8084–8087.

(22) Brothers, P.; Collman, J. The Organometallic Chemistry of Transition-Metal Porphyrin Complexes. *Acc. Chem. Res.* **1986**, 19, 209–215.

(23) (a) Bisel, P.; Al-Momani, L.; Müller, M. The *tert*-butyl Group in Chemistry and Biology. *Org. Biomol. Chem.* **2008**, 6, 2655–2665.

(b) DeGoey, D.; Randolph, J.; Liu, D.; Pratt, J.; Hutchins, C.; Donner, P.; Krueger, A.; Matulenko, M.; Patel, S.; Motter, C.; Nelson, L.; Keddy, R.; Tufano, M.; Caspi, D.; Krishnan, P.; Mistry, N.; Koev, G.; Reisch, T.; Mondal, R.; Pilot-Matias, T.; Gao, Y.; Beno, D.; Maring, C.; Molla, A.; Dumas, E.; Campbell, A.; Williams, L.; Collins, C.; Wagner, R.; Kati, W. Discovery of ABT-267, a Pan-Genotypic Inhibitor of HCV NS5A. *J. Med. Chem.* **2014**, 57, 2047–2057.

(24) Dong, Z.; MacMillan, D. W. C. Metallaphotoredox-enabled Deoxygenative Arylation of Alcohols. *Nature* **2021**, 598, 451–456.

(25) Chatgililoglu, C.; Griller, D.; Lesage, M. Rate Constants for the Reactions of Tris(trimethylsilyl)silyl Radicals with Organic Halides. *J. Org. Chem.* **1989**, 54, 2492–2494.

(26) Ogoshi, H.; Sugimoto, H.; Yoshida, Z.-I.; Kobayashi, H.; Sakai, H.; Maeda, Y. Synthesis and Magnetic Properties of Aryliron(III) Complexes of Octaethylporphyrins. *J. Organomet. Chem.* **1982**, 234, 185.

(27) (a) Kim, D. W.; Ahn, D.-S.; Oh, Y.-H.; Lee, S.; Kil, H. S.; Oh, S. J.; Lee, S. J.; Kim, J. S.; Ryu, J. S.; Moon, D. H.; Chi, D. Y. A New Class of  $S_N2$  Reactions Catalyzed by Protic Solvents: Facile Fluorination for Isotopic Labeling of Diagnostic Molecules. *J. Am. Chem. Soc.* **2006**, 128, 16394–16397. (b) Dongbang, S.; Doyle, A. Ni/Photoredox-Catalyzed  $C(sp^3)$ – $C(sp^3)$  Coupling between Aziridines and Acetals as Alcohol-Derived Alkyl Radical Precursors. *J. Am. Chem. Soc.* **2022**, 144, 20067–20077.

(28) Juliá, F.; Constantin, T.; Leonori, D. Applications of Halogen-Atom Transfer (XAT) for the Generation of Carbon Radicals in Synthetic Photochemistry and Photocatalysis. *Chem. Rev.* **2022**, 122 (2), 2292–2352.

(29) *Organosilanes in Radical Chemistry*, 1st ed.; Chatgililoglu, C., Ed.; Wiley-VCH: Weinheim, Germany, 2004.

(30) Hickman, D.; Shirazi, A.; Goff, H. Deuterium NMR Spectroscopic Studies of Low-Valent Iron Porphyrin Species. *Inorg. Chem.* **1985**, 24, 563–566.